A METHOD FOR DETECTING PHOTOVOLTAIC PANEL FAULTS USING A DRONE EQUIPPED WITH A MULTISPECTRAL CAMERA

Ran Duan[1] , Zhenling Ma[1,*]
AIEN Institute, Shanghai Ocean University, Shanghai, China , ran0704@qq.com, zlma@shou.edu.cn

KEY WORDS: Photovoltaic power stations, hot spot detection, UAVs, visible and infrared images.

ABSTRACT:
Photovoltaic power stations utilizing solar energy, have grown in scale, resulting in an increase in operational maintenance requirements. Efficient inspection of components within these stations is crucial. However, the large area of photovoltaic power generation, coupled with a substantial number of photovoltaic panels and complex geographical environments, renders manual inspection methods highly inefficient and inadequate for modern photovoltaic power stations. To address this issue, this paper proposes a method and system for hot spot detection on photovoltaic panels using unmanned aerial vehicles (UAVs) equipped with multispectral cameras. The UAVs capture visible and infrared images of the photovoltaic power plant, which are then processed for photogrammetry to determine imaging position and attitude. The infrared images are stitched together using this information, forming a geographically referenced overall image. Hot spot detection is performed on the infrared images, enabling the identification of faulty photovoltaic panels and facilitating efficient inspection and maintenance. Experimental trials were conducted at a photovoltaic power station in Qingyuan, Guangdong Province China. The results demonstrate the effectiveness of the proposed method in accurately detecting panels with hot spot faults.

1. INSTRUCTION

As the global economy advances, the demand for energy across nations continues to rise. Conventional fossil fuels like coal, oil, and natural gas are not only depleting but also produce carbon dioxide when burned, contributing to the greenhouse effect, global warming, and endangering life on Earth. Consequently, it has become a shared objective for countries to embrace sustainable, clean energy solutions. Among these, solar energy stands out as a clean, renewable, and limitless resource, promising to reshape the energy landscape and combat environmental challenges. Its potential has garnered significant attention globally (Ashok S., 2023 and Marta V., et al., 2021). Solar energy utilization, exemplified by photovoltaic power stations, has gained substantial traction and is actively expanding. However, the prolonged operation of photovoltaic array components in demanding conditions underscores the critical need for meticulous inspection within these power stations (Peng Z. et al., 2017). Notably, within photovoltaic power stations, one prevalent issue is the occurrence of hot spots, a typical fault in photovoltaic power generation systems. Research indicates that hot spots emerge when the current of a photovoltaic cell within a component diminishes due to obstructed sunlight. Consequently, the voltage at both ends of the affected cell drops, causing surrounding cells to supply it with charge. This turns the impacted cell into an "electrical load," continuously absorbing power from nearby cells and converting it into heat energy. As this heat accumulates, it can lead to destruction within the array due to excessive temperatures. Failure to promptly monitor and address a hot spot situation can result in damage to individual photovoltaic cells, potentially leading to their combustion and compromising the overall array, as depicted in Figure 1, which displays hot spots in an infrared image of a polycrystalline silicon photovoltaic array.

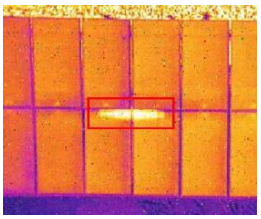

Figure 1. The hot spots in an infrared image

In the present context, prevalent detection methods encompass visual inspection, photoelectric excitation detection, volt-ampere detection, and infrared-based detection techniques. Visual inspection relies on human observation, either unaided or with the aid of devices, to visually examine solar panels and subjectively identify defects. However, this method proves impractical and perilous for extensive photovoltaic arrays and panels sited in hazardous locations, as it relies heavily on personnel experience and poses safety risks, ultimately leading to low detection efficiency (Ingeborg H. et al., 2022 and Q. Chen et al., 2023). Photoelectric excitation detection comprises photoluminescence and electroluminescence methods. These methods involve stimulating solar panels in a darkroom to generate a potential difference across the panel through photonic excitation. This process leads to electron collisions, resulting in radiation, with the detection image captured using specialized photosensitive components. Nonetheless, this approach necessitates additional circuits, rendering the operation complex and costly (Muhammad T. et al., 2020 and Chibane Y. et al., 2022). The volt-ampere detection method entails continually adjusting the resistance value of the photovoltaic system to derive the volt-ampere characteristics curve of the solar panel. Analysis of its variations aids in defect determination. However, this method demands measuring each individual photovoltaic panel, a task impracticable due to the expansive area of photovoltaic power generation and the substantial number of panels (M.W. Akram et al., 2022 and A. Mawjood et al., 2018).

The application of infrared imaging for detecting faults in photovoltaic (PV) modules has gained prominence recently. This method utilizes infrared devices to capture thermal images of PV systems. By analyzing the temperature distribution in

This contribution has been peer-reviewed. The double-blind peer-review was conducted on the basis of the full paper.
https://doi.org/10.5194/isprs-annals-X-1-2024-59-2024 | © Author(s) 2024. CC BY 4.0 License.

these images, the approach aims to identify hotspots within the PV module system. Notably, it showcases heightened detection efficiency compared to methods reliant on electrical characteristic monitoring and obviates the need for constructing peripheral physical circuits. As a non-contact hotspot detection method, it has become increasingly popular due to its minimal impact on PV modules. Nonetheless, the swift and precise acquisition of infrared images and accurate localization pose emerging challenges (Peng Z. et al., 2017 and Q. Chen et al., 2023).

The unmanned aerial vehicle (UAV) industry has rapidly evolved, integrating into the PV inspection domain due to its swift data acquisition and cost-effectiveness, effectively addressing the inspection challenges encountered in the PV sector. Several scholars, including H. Elidrissi, have delved into studies regarding the use of UAVs for PV plant inspections. These studies emphasize the pivotal role played by defect detection, identification, and on-site localization within the maintenance framework of solar PV installations, crucial for preserving their reliability and efficiency (H. Elidrissi, et al., 2022) .Peng Zhang and others have developed a drone-mounted infrared thermography system designed specifically for rapid fouling detection on large-scale PV panels. This system preprocesses infrared images using a K-nearest neighbor mean filter and applies a combined local and global detection method for precise location of suspicious sites, demonstrating a strong capability for detecting and pinpointing PV fouling (Peng Z. et al., 2017).

Furthermore, Nie and colleagues have presented a traditional image processing method combined with deep-learning-based techniques for hotspot detection in infrared images. Similarly, Liu J and Ji N have proposed a method for PV infrared image segmentation and hot spot location detection to identify and analyze PV panel shielding, irrespective of varying background conditions, thus enhancing detection accuracy and providing valuable data for power station maintenance (Nie J. et al., 2020 and Liu J and Ji N, 2023).

Meanwhile, Gurras A and team have introduced a new computational process for automated defect detection and classification on PV modules utilizing thermal imaging or IR thermography with assistance from UAVs. Their approach has proven to be a reliable and efficient tool for automated defect detection and classification (Gurras A, et al., 2021).

Moreover, M. Waqar Akram and associates have conducted research on automatic detection of photovoltaic module defects in infrared images using isolated deep learning and develop-model transfer deep learning techniques. Their work involves collecting an infrared image dataset comprising both normal operating and defective modules, which is then used to train the networks (M.W. Akram et al.,2020).

These advancements collectively underscore the evolving landscape of fault detection in PV systems, integrating cutting-edge technologies such as UAVs and infrared imaging, and employing sophisticated methods including deep learning to ensure the continued efficiency and reliability of photovoltaic power generation (D.L.King et al., 2000 and S. Dotenco et al., 2016 and Grimaccia F. et al., 2017).

In conclusion, despite the extensive research conducted on drone-based photovoltaic (PV) plant inspection systems, these endeavors intersect different domains, including drone technology, image processing, and data analysis, necessitating thorough research and innovative solutions. Presently, this system grapples with persistent challenges such as the precision of drone image positioning and timely identification of hotspots in infrared images. This paper consolidates and enhances existing research by leveraging diverse methodologies to engineer a more pragmatic and user-friendly drone-based inspection system tailored for real-world application needs. Additionally, it delves into the exploration of algorithms for hotspot detection, intending to offer guidance and inspiration for future research in this domain. The contributions of this paper are outlined as follows:

1)A method for obtaining the overall infrared image of photovoltaic panels was proposed using drones equipped with visible light cameras and infrared cameras. Based on the fundamental principles of photogrammetry, this method involves the directional processing of visible light images, the application of the obtained exterior orientation elements to the infrared images, and the subsequent stitching of the infrared images to acquire the overall geographic information of the photovoltaic panels.

2)A hot spot extraction method based on Otsu's thresholding and morphological processing was proposed for extracting hot spots from the obtained overall infrared images, thereby achieving fault detection in photovoltaic panels.

3)An experiment was conducted at a photovoltaic power station in Qingyuan City, Guangdong Province, China, to validate the effectiveness of this method.

2. METHODOLOGY

The proposed methodology aims to address the issue of low efficiency in photovoltaic module inspections. It suggests using unmanned aerial vehicles (UAVs) equipped with multispectral cameras for thermal spot detection of photovoltaic panels. The process begins with UAV aerial photography of the photovoltaic power plant, capturing both visible and infrared images. The visible light images undergo photogrammetric processing to determine imaging positions and attitudes. These parameters are then used to stitch together the infrared images, creating a geographically referenced composite image. Finally, thermal spot detection is performed on the infrared images to identify problematic photovoltaic panels, streamlining inspection and maintenance. You can refer to Figure 2 for a visual representation of the system's workflow.

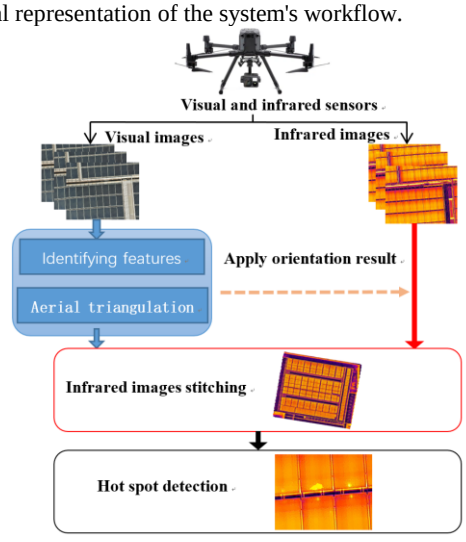

Figure 2 The system's workflow of the paper

2.1 Infrared Images Stitching

Although current unmanned aerial vehicles (UAVs) are equipped with POS systems that can directly obtain the position and attitude of captured images, this information alone is insufficient for precise positioning and Mosaicking of the images. Therefore, professional photogrammetric processing is

required to accurately determine the parameters of the images and generate a georeferenced composite image. Since infrared images have smaller footprints and lack distinct features compared to visible light images, direct photogrammetric processing is not feasible. Hence, this paper first applies photogrammetric processing to the visible light images to obtain precise POS at the time of capture, which is then applied to the infrared images to generate a composite image of the infrared data.

The precise parameter estimation of UAV imagery in photogrammetry is referred to as aerial triangulation, which is a well-established technique in the field. The core process involves automatic matching of corresponding points in the images and bundle adjustment of the image block. In the field of computer vision, this technique is also known as Structure from Motion (SFM), which aims to solve the camera's position and orientation and reconstruct the 3D scene based on the image relationships. The key steps in aerial triangulation include obtaining corresponding points between multiple images through feature matching and minimizing the reprojection error of the feature points to solve for the image projection matrix, camera intrinsic parameters, and the 3D coordinates of the feature points. The specific process involves selecting a pair of images for relative orientation, gradually adding images with overlapping areas to the model, performing adjustment and updating the 3D points, until all images are included to complete the block adjustment. This process is illustrated in Figure 3.

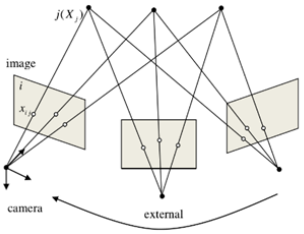

Figure 3 SFM’s process

The processing steps for Structure from Motion (SFM) are as follows:

1)Establish image adjacency relations (using GPS/POS assistance or image retrieval methods).

2)Select a pair of images with relatively numerous adjacency relations from the adjacency relation table as the first image pair.

3)Carry out feature matching for the first image pair to obtain tie points. Use the decomposition of the essential matrix to calculate the exterior orientation elements of the image pair and the object space coordinates of the tie points, forming the current model.

4)Choose an image adjacent to the current model, and match tie points in the current model with the image. Use the 3D coordinates of the tie points in the current model to calculate the exterior orientation elements for the new image.

5)Use intersection to solve for the object space coordinates of newly added tie points.

6)If the number of tie points exceeds a predetermined threshold (e.g., conduct adjustment for every additional 2000 points), then perform a global bundle adjustment for the existing model.

7)Repeat steps 4),5),6) until all images have been processed.

The central aspect of this process involves identifying identical features in each pair of photos. SIFT, proposed by D.G. Lowed in 1999 and later refined and summarized in 2004, is among the most widely used algorithms for this purpose. It searches for extrema across spatial scales and captures their position, scale, and rotational invariance. SIFT features denote local extrema in an image's scale space, distinct from nearby points within the same area and scale, representing peaks or troughs of the local differential Gaussian function within the image. SIFT feature points appear as areas with grayscale values either higher or lower than those of the surrounding and neighboring points within the same area and scale. Thus, the SIFT algorithm can be viewed as a method for extracting interest points based on grayscale variations (D.G. Lowe,1999 and D.G. Lowe,2004.).

The second important step involves identifying the transformation. There exist numerous types of geometric transformations, with one of the most widely used being Sparse Bundle Adjustment(SBA). Its core lies in optimizing camera parameters and three-dimensional point coordinates using the Levenberg-Marquardt algorithm, wherein the primary process begins with establishing imaging relationships (M. Brown, D.G. Lowe, 2005 and M. Lourakis, A. Argyros, 2004.)

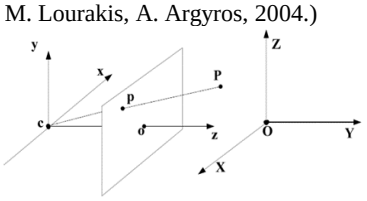

Figure 4 The principles of imaging geometry

As shown in the figure 4, the object point P is projected to the image point p on the image plane. Assuming the coordinates of the object point in the object space coordinate system are $\bar{X}$ = (X, Y, Z), and the coordinates of the image point p in the image space coordinate system are $\bar{x}$ = (x, y, z), then

$$\bar{x} = R\bar{X} + \bar{t}$$

In the formula, $\bar{t}$ is a translation(dX,dY,dZ) from real coordinates and R represents the rotation matrix, that is:

$$R = e^{[\theta]}, [\theta] = \begin{bmatrix} 0 & -\theta_3 & \theta_2 \\ \theta_3 & 0 & -\theta_1 \\ -\theta_2 & \theta_1 & 0 \end{bmatrix}$$

The θ_1, θ_2,θ_3 is three angle rotation with X,Y,Z axis.

Every feature point corresponds to an object point X_j. The error equation for the bundle adjustment of sparse bundle adjustment is the sum of the squares of the image point errors for all object points in the corresponding images, that is:

$$e = \sum_{i \in I} \sum_{j \in \chi(i)} f(\bar{r}_{ij})^2$$

Where I denotes all the images, χ(i) represents the list of t object points corresponding to image i. Assuming the reprojected image point of point X_j in image i is $\bar{u}_{ij}$, and the corresponding feature point is $\bar{m}_{ij}$, the image point error is:

$$\bar{r}_{ij} = \bar{m}_{ij} - \bar{u}_{ij}$$

The iterative equation solved using the Levenberg-Marquardt algorithm is:

$$\bar{\Phi} = (J^T J + \sigma^2 C_p^{-1})^{-1} J^T \bar{r}$$

Where $\bar{\Phi}$ = [Θ, X] is the vector of camera parameters Θ and feature point coordinates X, $\bar{r}$ is the residual vector, σ is three times the standard error, J = ∂r/∂Φ is an M × N matrix (M is the number of images, N is the number of unknowns to be solved), and J also known as the Jacobian matrix, and C is the covariance matrix. In this study, the Ceres Solver framework is directly used to solve for obtaining the image projection matrix, camera intrinsic parameters, and feature point object space coordinates.

After obtaining precise parameters from the images, they are directly applied to the infrared images. Firstly, a digital terrain model (DTM) is generated using the 3D points. Then, the infrared images are projected onto the ground using the imaging

equation, creating multiple orthophoto, which are joined based on their geographical locations. The stitching process employs the "Voronoi diagram" algorithm to select the best-fitting images. The algorithm is described as follows:
1)Compute the centroids of each orthophoto, and use them as nodes of the Voronoi diagram.
2)Use the set of all nodes to construct a Delaunay triangulation.
3)Obtain the valid areas of each orthophoto based on the Delaunay triangulation.
4)Fill in data based on the valid area of each image.

2.2 Hot spot detection

After obtaining georeferenced whole infrared images, spot detection is initiated. Due to the characteristic of spots being of higher temperature, the average value of the infrared image is used as a threshold, filtering out positions with temperatures lower than the average. Subsequently, OTSU’s method for binarization and morphological processing is employed to extract the spot locations. For the processing principle of OTSU, please read Otsu’s paper (Otsu, N. 1979 and Bangare, S. et al., 2015). After OTSU processing, the result shown in Figure 5 can be obtained.

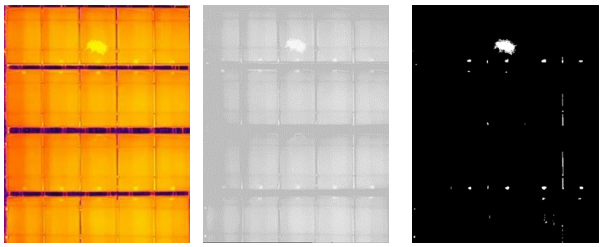

(a) (b) (c)

Figure 5 The binarization filtering and results: (a)Source Infrared image (b) Filtering by the average temperatures (c) The results of OTSU

As shown in Figure 5, the surface defect image of the photovoltaic panel retains only the surface defects and the most prominent grid lines. Some finer grid lines have been removed. While some details of the defects are preserved, they are not finely detailed enough. Consequently, this paper applies morphological processing to the image. Morphological processing typically includes opening and closing operations. Opening operation involves erosion followed by dilation. Its primary function is to separate certain loosely connected elements in the image, while simultaneously being able to remove tiny details in the image. Closing operation involves dilation followed by erosion. Its purpose is to connect adjacent but not yet touching objects while also filling in the cavities in the image. The image obtained after morphological processing of Morphological processing is shown in Figure 6.

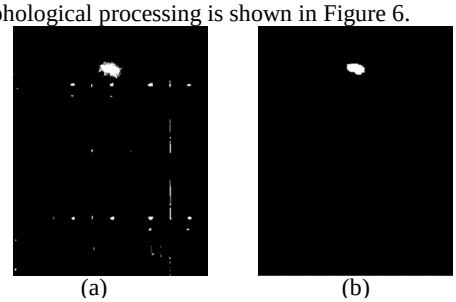

(a) (b)

Figure 6 Morphological processing: (a) The input data(results of OTSU) (b) Morphological results

Clearly, this is the glare that we ultimately hope to obtain, and based on the glare's position, we can identify problematic solar panels.

3. EXPERIMENTAL RESULTS

3.1 Research materials

This paper selects a small area of a photovoltaic power station located in Qingyuan City as the research object. The planned total installed capacity of the photovoltaic power station is 500MW, and the total land area is 5,167,100 square meters. The voltage level is 220kV. After all the photovoltaic arrays in the photovoltaic area are built, the annual grid-connected electricity generation is 58,350.5 MWh, and the annual equivalent full-load operation hours are approximately 1167 hours.
The experiment uses the DJI M300 unmanned aerial vehicle as the flight platform, equipped with the Zenmuse H20T dual-camera to capture visible light and infrared images of the photovoltaic power station. The specific images and parameters of the equipment are as Figure 7 and Table 1.

(a) (b)

Figure 7 Image of equipment: (a)DJI-M300 drone and (b)H20T dual-camera

Table 1 Technical specifications of H20T dual-camera

	Infrared	Visible
Image Resolution	640×512pixels	4056×3040pixels
Pixels Size	12 μm	3.67μm
Focus Length	13.5 mm	4.5mm
Image Format	R-JPEG (16 bit)	JPEG(8 bit)
DFOV	40.6 °	82.9°
GPS Info	Yes	Yes
Gimbal Info	Yes	Yes

The H20T dual-camera system simultaneously captures visible light and infrared images. In this experiment, a total of 3767 visible light images and their corresponding 3767 infrared images were obtained over 9 sorties, with some sample images shown in Figure 8 and Figure 9.

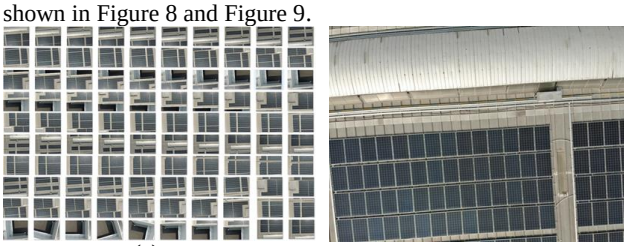

(a) (b)

Figure 8 Visible light images: (a)The thumbs of visible light images (b)A visible light image

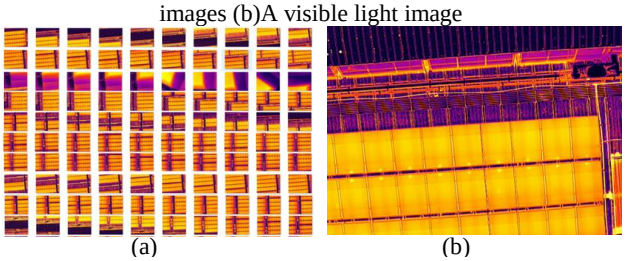

(a) (b)

Figure 9 Infrared images: (a)The thumbs of infrared images (b)An infrared light image

Due to the different image dimensions of visible light and infrared images from the H20T system, overlaying two images acquired at the same time results in the visualization shown in Figure 10.

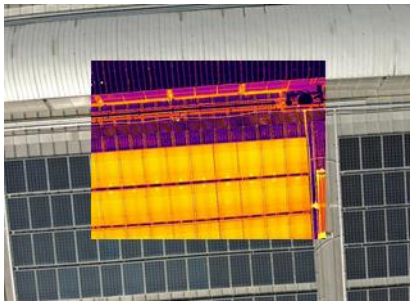

Figure 10 Overlaying of visible light image and infrared image

3.2 Infrared Images Stitching Results

Following the method outlined in section 2.1, we initially conducted aerial triangulation processing on the 3767 visible light images, obtaining image spatial position, orientation, and corresponding three-dimensional point information as depicted in Figure 11.

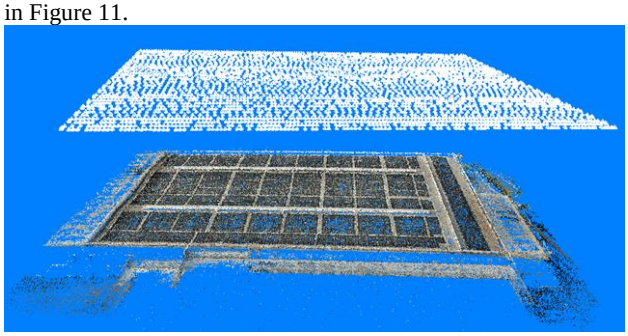

Figure 11 Aerial triangulation result for visible light images

Directly applying the spatial position and orientation of the visible light images to the infrared images, the resulting infrared images were overlaid onto a digital surface model, as shown in Figure 12

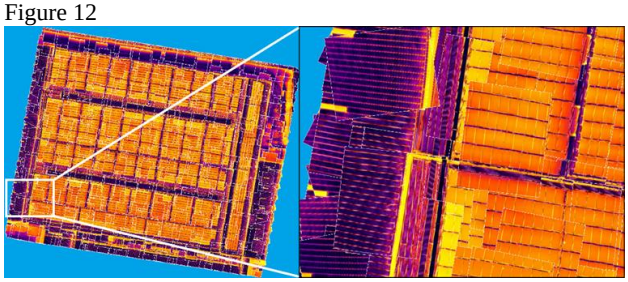

(a) (b)

Figure 12 Overlaping view by orientation of the visible light images for all infrared images: (a)Overlaping all view (b)The part of all view

Utilizing the ground points information obtained from the visible light images, a ground elevation model was generated. Using a ground resolution of 0.1 meters for the infrared images, an overall infrared orthophoto image produced through the "Voronoi diagram" algorithm described in section 2.1 is presented in Figure 13

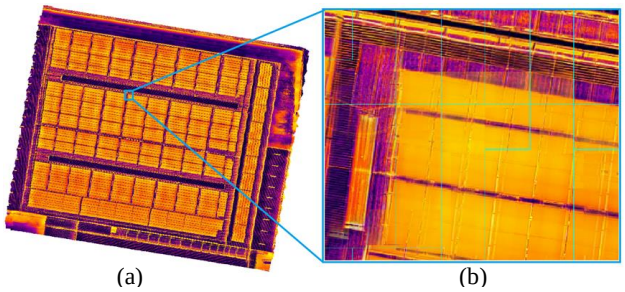

(a) (b)

Figure 13 The stitching results of infrared images: (a)All image (b)The part of all image and cyan lines is seamline

3.3 Hot spot detection results

After obtaining the overall infrared orthophoto image, based on the design data of the photovoltaic power station, we segmented out corresponding infrared orthophoto images based on the geographic coordinates of each photovoltaic panel, resulting in 110 groups named 1 to 110, as illustrated in Figure 14.

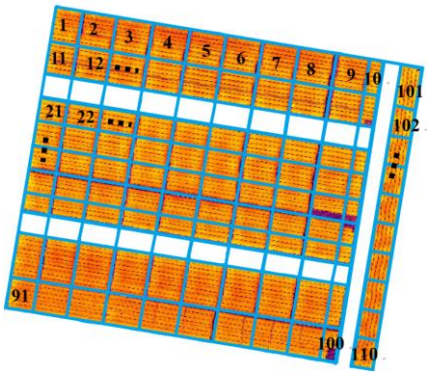

Figure 14 Infrared orthophoto image and segment to groups

Subsequently, employing the method described in section 2.2, Otsu's binarization and morphological processing were carried out for each group of photovoltaic panels. Most groups did not show any anomalies, while the processing results for panels numbered 20 and 60 are depicted in Figure 15.

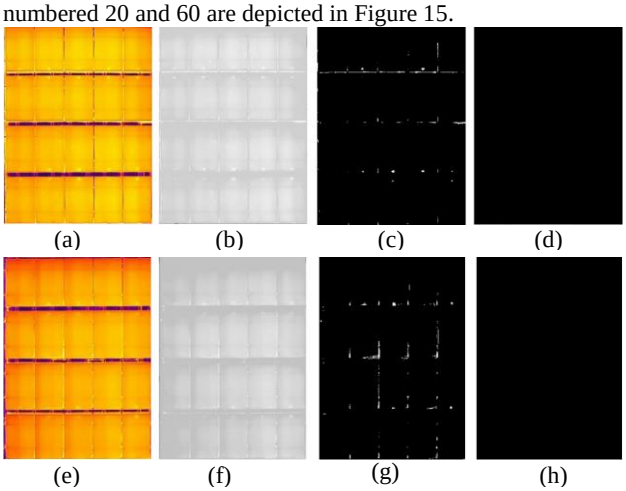

(a) (b) (c) (d)

(e) (f) (g) (h)

Figure 15 Cases for don't find hot spots: (a)(e)Source infrared image (b)(f) Filtering by the average temperatures (c)(g) The results of OTSU (d)(h) Morphological results(nothing in black)

Notably, panels with conspicuous bright spots were also identified, particularly panel number 10, as shown in Figure 16.

This contribution has been peer-reviewed. The double-blind peer-review was conducted on the basis of the full paper.
https://doi.org/10.5194/isprs-annals-X-1-2024-59-2024 | © Author(s) 2024. CC BY 4.0 License.

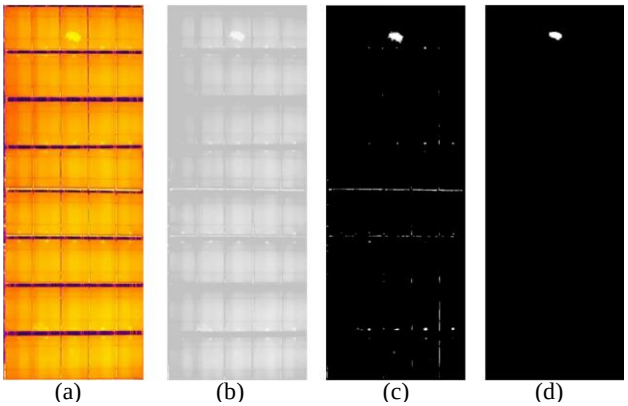

(a) (b) (c) (d)

Figure 16 Case for find a hot spot: (a) Source infrared image (b) Filtering by the average temperatures (c) The results of OTSU (d) Morphological results

To verify the accuracy of the detection results, we conducted a current-voltage (IV) characteristic test on the photovoltaic panels where bright spots were observed. The results showed that the panel associated with group 10 was not working properly and indeed required replacement. The visible light image of component 10 is depicted in Figure 17.

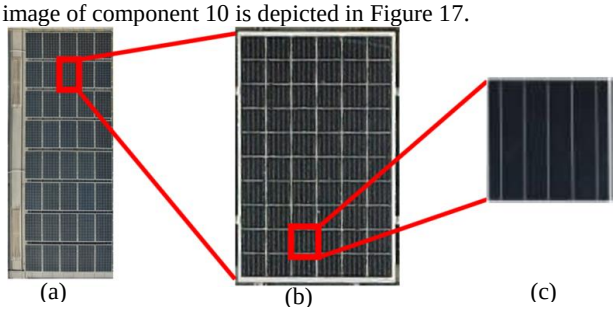

(a) (b) (c)

Figure 17 Visible light image for a photovoltaic panel faults

Additionally, at the location of photovoltaic component 90, two bright spots were detected and labeled as A and B. The processing procedure for these spots is illustrated in Figure 18.

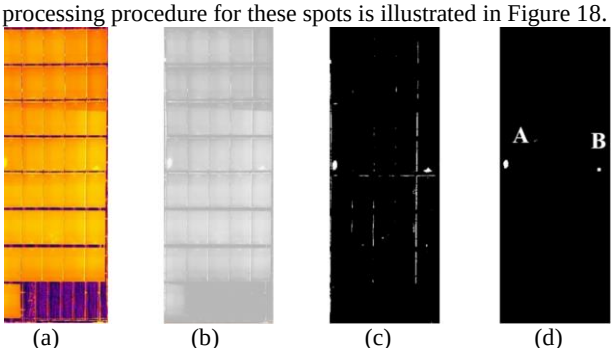

(a) (b) (c) (d)

Figure 18 Case for find two hot spot: (a) Source infrared image (b) Filtering by the average temperatures (c) The results of OTSU (d) Morphological results(Two hot spot)

Similarly, the IV characteristic test was carried out at positions A and B, leading to the determination that the photovoltaic panel at position A was malfunctioning and needed replacement, while the IV characteristics of the panel at position B did not indicate any obvious abnormalities and could continue to be used. It should be noted that for small bright spots, their accuracy in detection may be somewhat reduced.

4. CONCLUSION

This paper proposes a method and system for using drones equipped with multispectral cameras to conduct hotspot detection on photovoltaic panels, addressing the issue of low efficiency in photovoltaic module inspections. Through experiments conducted at a solar photovoltaic power station in Qingyuan, Guangdong Province, the results show that the proposed photovoltaic panel hotspot detection method is highly effective, facilitating efficient detection of faulty photovoltaic panels with hotspots. In comparison to traditional methods, this approach has several advantages. Firstly, it only requires aerial photography using drones, eliminating the need for physical contact measurement on the photovoltaic panels, making it not only convenient and economical but also operationally simple. Secondly, it is highly efficient, with both the photographic and detection processes being fully automated. Lastly, the method results in minimal missed detections, ensuring the normal temperature of the photovoltaic panels. However, there are areas in this method that require further optimization, such as determining the appropriate hotspot size to reduce false detection rates while ensuring no missed detections.

ACKNOWLEDGEMENTS

This study was supported by National Natural Science Foundation of China Youth Fund, No. 42101443 (Construction of Semi parametric Geometric Model for Multi medium Refraction in Underwater Optical Images).

REFERENCES

Ashok S., 2023. Solar energy. Encyclopedia Britannica, 22 Dec. 2023, https://www.britannica.com/science/solar-energy. Accessed 23 December 2023.

Marta V., et al., 2021. Solar photovoltaics is ready to power a sustainable future, Joule,Volume 5, Issue 5,2021,Pages 1041-1056,ISSN 2542-4351, doi.org/10.1016/j.joule.2021.03.005..

Peng Z., et al., 2017. Detection and location of fouling on photovoltaic panels using a drone-mounted infrared thermography system, J. Appl. Rem. Sens. 11(1) 016026 (11 February 2017).

Ingeborg H. et al., 2022. Inspection and condition monitoring of large-scale photovoltaic power plants: A review of imaging technologies, Renewable and Sustainable Energy Reviews, Volume 161,2022, 112353, ISSN 1364-0321, doi.org/10.1016/ j.rser.2022.112353.

Qi Chen, et al., 2023. Remote sensing of photovoltaic scenarios: Techniques, applications and future directions, Applied Energy,Volume 333,2023,120579,ISSN 0306-2619,doi.org/10.1016/ j.apenergy.2022.120579..

Muhammad T. et al., 2020. Environmental impacts of solar photovoltaic systems: A critical review of recent progress and future outlook, Science of The Total Environment, Volume 759, 2021,143528,ISSN 0048-9697,doi.org/10.1016/j.scitotenv.2020.143528.

Chibane Y., et al., 2022. Application of Electroluminescence Technique to the Characterization of Conventional Solar Cells. doi.org/10.13140/RG.2.2.31048.80642/1.

M. Waqar Akram,et al., 2022. Failures of Photovoltaic modules and their Detection: A Review,Applied Energy,Volume

313,2022,118822,ISSN 0306-2619, doi.org/10.1016/j.apenergy.2022.118822.

K. AbdulMawjood, et al., 2018. Detection and prediction of faults in photovoltaic arrays: A review, 2018 IEEE 12th International Conference on Compatibility, Power Electronics and Power Engineering (CPE-POWERENG 2018), Doha, Qatar, 2018, pp. 1-8, doi: 10.1109/CPE.2018.8372609.

H. Elidrissi, et al., 2022. Automatic on Field Detection and Localization of Defective Solar Photovoltaic Modules from Orthorectified RGB UAV Imagery, 2022 6th International Conference on Green Energy and Applications (ICGEA), Singapore, Singapore, 2022, pp. 46-50, doi: 10.1109/ICGEA54406.2022.9791946.

Nie J., et al., 2020. Automatic hotspots detection based on UAV infrared images for large-scale PV plant. Electron. Lett., 56: 993-995. doi.org/10.1049/el.2020.1542.

Liu J and Ji N, 2023. A bright spot detection and analysis method for infrared photovoltaic panels based on image processing. Front. Energy Res. 10:978247. doi: 10.3389/fenrg.2022.978247.

Gurras A, et al., 2021. Automated detection-classification of defects on photo-voltaic modules assisted by thermal drone inspection[J]. 2021. doi:10.1051/matecconf/202134903015.
M. Waqar Akram, et al.,2020. Automatic detection of photovoltaic module defects in infrared images with isolated and develop-model transfer deep learning,Solar Energy,Volume 198,2020,Pages 175-186,ISSN 0038-092X, doi:10.1016/j.solener.2020.01.055.

D.L.King, et al., 2000. Applications for infrared imaging equipment in photovoltaic cell, module, and system testing, Conference Record of the Twenty-Eighth IEEE Photovoltaic Specialists Conference - 2000 (Cat. No.00CH37036), Anchorage, AK, USA, 2000, pp. 1487-1490, doi: 10.1109/PVSC.2000.916175.

S. Dotenco et al., 2016. Automatic detection and analysis of photovoltaic modules in aerial infrared imagery, 2016 IEEE Winter Conference on Applications of Computer Vision (WACV), Lake Placid, NY, USA, 2016, pp. 1-9, doi: 10.1109/WACV.2016.7477658.

Grimaccia F, et al., 2017. PV plant digital mapping for modules’ defects detection by unmanned aerial vehicles[J]. Iet Renewable Power Generation, 2017, 11(10): 1221-1228.

D.G. Lowe,1999. Object Recognition from local scale-Invariant Features．7th International conference on Computer Vision［C］．1999：1150-1157．

D.G. Lowe,2004. Distinctive Image Feature form Scale-invariant Keypoints[J]. International Journal of Computer Vision，2004，60(2)：91-110．

M. Brown, D.G. Lowe, 2005. Unsupervised 3D object recognition and reconstruction in unordered dataset. In: Proceedings of the international conference on 3D digital imaging and modelling[C].2005:56-63

M. Lourakis,A. Argyros, 2004. The Design and Implementation of a Generic Sparse Bundle Adjustment Software Package based on the LM Algorithm．FORTH-ICS Technical Report，TR-340，2004．

Otsu, N. 1979. A Threshold Selection Method from Gray-Level Histograms. IEEE Trans. Syst. Man Cybern. 9 (1979): 62-66.

Bangare, S. et al., 2015. Reviewing Otsu’s Method For Image Thresholding. International Journal of Applied Engineering Research. 10. 21777-21783. doi:10.37622/IJAER/10.9.2015.21777-21783.

Roberto A, et al., 2023. Chapter Six - Morphological Image Processing,Editor(s):Fatima A. Merchant, Kenneth R. Castleman,Microscope Image Processing (Second Edition), Academic Press, 2023, Pages 75-117,ISBN 9780128210499, doi.org/10.1016/B978-0-12-821049-9.00012-5.